Joint energy consumption optimization method for wing-diesel engine-powered hybrid ships towards a more energy-efficient shipping

Wang, Kai; Xue, Yu; Xu, Hao; Huang, Lianzhong; Ma, Ranqi; Zhang, Peng; Jiang, Xiaoli; Yuan, Yupeng; Negenborn, Rudy R.; Sun, Peiting

DOI
10.1016/j.energy.2022.123155

Publication date
2022

Document Version
Final published version

Published in
Energy

Energy 245 (2022) 123155

Contents lists available at ScienceDirect

Energy

journal homepage: www.elsevier.com/locate/energy

Joint energy consumption optimization method for wing-diesel engine-powered hybrid ships towards a more energy-efficient shipping

Kai Wang [a], Yu Xue [a], Hao Xu [a], Lianzhong Huang [a, *], Ranqi Ma [a, **], Peng Zhang [a], Xiaoli Jiang [b], Yupeng Yuan [c, d], Rudy R. Negenborn [b], Peiting Sun [a]

[a] Marine Engineering College, Dalian Maritime University, Dalian, 116026, China
[b] Faculty of Mechanical, Maritime and Materials Engineering, Delft University of Technology, Mekelweg 2, Delft, 2628 CD, Netherlands
[c] Department of Engineering, University of Cambridge, Cambridge, CB3 0FA, UK
[d] National Engineering Research Center for Water Transport Safety (WTSC), MOST, Wuhan, 430063, China

ARTICLE INFO

Article history:
Received 18 June 2021
Received in revised form
7 November 2021
Accepted 7 January 2022
Available online xxx

Keywords:
Hybrid ship
Energy consumption optimization
Wind energy
Low carbon shipping
Carbon neutrality

ABSTRACT

Wing-diesel engine-powered hybrid ships can effectively reduce fuel consumption and CO_2 emissions by using wind energy as the auxiliary driving power. The energy optimization management of the hybrid system can further improve the ship's energy efficiency. To achieve this purpose, it is significant to establish an effective energy consumption model for the energy optimization management of the hybrid system. Therefore, an energy consumption model is established based on the energy conversion analysis of the hybrid power system in this paper. This model can effectively describe the energy consumption of the hybrid ship under different navigational environmental conditions. Then, a joint optimization method of the wing attack angle and of the sailing speed for the hybrid ship is proposed by adopting a swarm intelligence optimization algorithm, in order to reduce energy consumption and CO_2 emissions of the hybrid ship under different navigational environmental conditions. Finally, the energy consumption optimization potentials by adopting the hybrid power system and the proposed joint optimization method are analyzed. The results show that the energy consumption and CO_2 emissions along a typical route can be reduced by about 4.5%. This study provides an important basis for future practical operations of wing-diesel engine-powered hybrid ships.

1. Introduction

The shipping industry plays an important role in promoting the development of world trade. However, with the continuous increase of the transport volume and the common use of heavy fuel oil, some serious problems (e.g., energy shortages and abundant pollution gas emissions) have emerged [1]. Under these conditions and the increasing attention of the international community to energy conservation and emission reduction, the application of new, clean types of energy has become an urgent issue [2]. As a matter of fact, the increasingly strict emission reduction measures proposed by the International Maritime Organization (IMO) and many governments worldwide have accelerated the development and application of such energy in the shipping industry [3]. The utilization of renewable energy (e.g., wind [4] and solar [5] energy) is fundamental for realizing a green and sustainable development of this field [6]. For instance, wind energy has shown good potential in relation to sea-going ships, due to its abundance and low cost for practical applications. Data regarding the world's first sail-assisted commercial vessel, "Shin-Aitoku-Maru", have shown that 20%–30% of the original fuel can be saved along specific sailing routes [7]. The application of wind energy (through wing-diesel engine-powered hybrid systems in which the wing is used as an auxiliary power source), can also effectively reduce pollution gas emissions [8]. Overall, sea-going vessels can effectively achieve both energy conservation and emission reduction by adopting wing-diesel engine-powered hybrid power systems [9].

Rigid-wing sails have the best aerodynamic characteristics (e.g.,

* Corresponding author.
** Corresponding author.
E-mail addresses: huanglz@dlmu.edu.cn (L. Huang), maranqi1989@dlmu.edu.cn (R. Ma).

https://doi.org/10.1016/j.energy.2022.123155
0360-5442/

a high aerodynamic lift coefficient, a wide application range of wind directions, and a simple structure) among all types of sails and, hence, have a good application prospect [10]. The working characteristics of sails have as well an important impact on their working efficiency and, thus, influence the utilization efficiency of wind energy [11]. The design optimization of rigid-wing sails for wing-diesel engine-powered hybrid ships has been studied previously [10]. It was found that the aerodynamic optimization of the wing can be realized by applying the parametric section airfoil parameterization (PARSEC) method and the particle swarm optimization (PSO) algorithm. A coupled wing design based on the American National Advisory Committee for Aeronautics (NACA) airfoil and an arc-shaped wing optimized based on the PARSEC and the PSO algorithm have been shown to have better aerodynamic characteristics, with power factors 25.04% higher than that of a traditional coupling wing [10]. Notably, the auxiliary driving force coefficient of a wing is influenced by its structure and aerodynamic characteristics [12]. This coefficient can hence be improved by optimizing the wing's shape [13]. A wind tunnel test has been conducted on wings of different shapes, verifying that a variable bending wing can provide greater thrust compared to other types of wings [14]. The optimal performance coefficient and the attack angle of a wing model have been analyzed according to the results of a wind tunnel test [15], providing a solid foundation for further research and the application of new types of rigid-wing sails.

The application of wing sails requires the wind within the navigational area to meet certain characteristics, including an appropriate wind speed and a stable wind direction [16]. However, the wind fields in the ocean environment are complex and wind energy resources have obvious spatial−temporal differences. In addition, during ship navigation, energy consumption is influenced by numerous factors: winds, waves, currents, and other multi-navigational environmental factors. These factors have strong spatial−temporal differences and variabilities, making it very complex to analyze the navigational state, the wings' operational state, and the working characteristics of the propulsion system under different navigational conditions [17]. Therefore, it is necessary to analyze the characteristics of the navigational environment (especially the wind energy resources) and their influence on the ship's energy consumption. The energy transferring relationship for a propulsion system under different conditions has been analyzed in a previous work [18], establishing a propulsion system model. On this basis, the dynamic characteristics of the propulsion system can be analyzed and predicted [19]. The relationships between fuel consumption, the navigational environment, and the heading course of a ship have been analyzed in Ref. [20], proposing a semi-empirical prediction model of the operational performance that can predict the operational state of a ship under different draught, speed and course conditions. Moreover, an alternating sparse self-coding network model has been established in Ref. [21], and the influence of the marine environment on the sailing speed has been analyzed on its basis. In addition, a mathematical model incorporating a ship, its main engine, propeller, and wings has been established in Ref. [22] through the analysis of the wing thrust characteristics, the propeller characteristics, the ship resistance, and the diesel engine power output characteristics. This model has been used to realize an analysis of the disturbance caused by the installed wings to the diesel engine. The computational fluid dynamics (CFD) method has also been used to establish a dynamics model of a wing-diesel engine-powered hybrid power system. In particular, a Reynolds-averaged Navier−Stokes computational fluid dynamics (RANS-CFD) method has been proposed to analyze the hydrodynamics of wind-assisted ships operating at leeway angles [23]. Existing studies, however, have not yet established an energy consumption model capable of comprehensively considering the wing thrust, propeller, ship resistance, and diesel engine power output characteristics of a wing-diesel engine-powered hybrid ship. Therefore, it is still difficult to predict the energy consumption level of a hybrid ship under different wind energy resources and navigational environmental conditions.

The optimal management of the wing-diesel engine-powered hybrid power systems would effectively improve ships' energy efficiency [24]. In this view, it is important to study a method for the optimization of the propulsion system's and wings' operational state under different navigational conditions [25]. The thrusts of the propeller and of the wing required for achieving a certain cruising speed were analyzed and calculated; moreover, the optimal operational state of the wing under different wind conditions has been analyzed to maximize the wing's thrust and reduce that of the propeller [26]. In another work [27], the energy-saving effect obtained through an optimal control of the sail's angle under different wind speeds and directions was evaluated. Furthermore, in Ref. [28], a route optimization algorithm of sail-installed ships has been studied based on the minimum fuel consumption and shortest route model, according to the distribution characteristics of wind energy resources along typical sailing routes. The great significance of achieving the operational optimization of wing-diesel engine-powered hybrid systems (to make full use of wind energy resources) has been confirmed through a wind energy analysis [29]. In order to maximize the use of wind energy resources and reduce fuel consumption, the navigation optimization of wing-diesel engine-powered hybrid ships can be realized by adopting a new artificial potential field-based passive navigation algorithm [30] and a fuzzy logic-based parallel navigation algorithm [31]. Although these optimization methods for the wing-diesel engine-powered hybrid power systems can effectively reduce a ship's fuel consumption, existing research has not focused on the dynamic influence of the wing on the working state of the diesel engine; in addition, the energy efficiency of a hybrid ship is not only influenced by the wing's working state, but also by the diesel engine's working load [32]. Therefore, a joint optimization of the wing attack angle and of the engine speed can further improve the ship energy efficiency. To the best of our knowledge, few studies have focused on the speed optimization of wing-diesel engine-powered hybrid ships, and particularly on the joint optimization mentioned above.

In this study, to improve ships' energy efficiency and reduce their CO_2 emissions, we established a method for the joint optimization of the wing attack angle and of the sailing speed of wing-diesel engine-powered hybrid ships. Our main contributions are listed below. 1) An energy consumption model of wing-diesel engine-powered hybrid power systems was established. This model comprehensively considers the wing thrust, propeller, ship resistance, and diesel engine working characteristics. Notably, it can effectively describe the fuel consumption of wing-diesel engine-powered hybrid ships under different wind energy resources and navigational environmental conditions, laying a solid foundation for future research on fuel consumption optimization in wing-diesel engine-powered hybrid ships. 2) A joint optimization of the wing attack angle of the sailing speed of wing-diesel engine-powered hybrid ships was proposed. This optimization was based on a temporal−spatial characteristics analysis of the wind energy resources within the navigational area. The results showed that the proposed joint optimization method can effectively reduce the fuel consumption and, thus, the CO_2 emissions of wing-diesel engine-powered hybrid ships. Overall, the findings of this work provide an important basis for future practical operations and the management of wing-diesel engine-powered hybrid ships.

The remaining parts of this paper are as follows. The

configuration design of the wing-diesel engine-powered hybrid power system is illustrated in **Section 2**. Then, an energy consumption model of wing-diesel engine-powered hybrid ships is established in **Section 3**. Afterwards, a joint optimization method of the wing attack angle and of the sailing speed under different wind energy resources and navigational conditions is proposed in **Section 4**. On these bases, the optimization results analysis and discussions for a typical route are carried out in **Section 5**. Finally, the conclusions and the future research work are given in **Section 6**.

2. The configuration design of the wing-diesel engine-powered hybrid power system

The configuration design of the wing-diesel engine-powered hybrid power system is illustrated in Fig. 1. The diesel engine and the wings collaboratively provide power to overcome the ship's sailing resistance. When the navigational environment is suitable for the wings' application, the wings would be raised to provide auxiliary driving force and, thus, decrease the output power of the main diesel engine of the hybrid ship. Therefore, the application of the wings can effectively reduce energy consumption of the ship. However, the magnitude and direction of the driving force of the wings vary with the wind characteristics and the wings' angles-of-attack. In order to improve the utilization efficiency of the wind energy, it is necessary to collect the real-time wind energy information and to achieve the optimization control of the wings' operational state under different working conditions.

At present, most of the wing-type sails are telescopic and can be raised and lowered to fit the wind conditions. The wings and the main diesel engine can be controlled on the bridge or in the central control room. When the navigational environment is not suitable, the wings cannot be used and then the diesel engine would be used as the single power source. In this way, it can ensure the safety of the ship's navigation. Through the perception and calculation of the sailing status, navigational environment and the energy consumption model, the energy consumption of the hybrid ship can be predicted and evaluated. In addition, the energy consumption optimization of the hybrid power ship can be achieved by establishing a joint optimization model of the wing attack angle and of the sailing speed. On the bases of the distribution characteristics analysis of the wind energy resources and the energy consumption model of the ship, the wing attack angles and sailing speeds under different working conditions can be jointly optimized, thus to reduce the fuel consumption and CO_2 emissions. Therefore, the wind energy resources analysis and the energy consumption optimization model are the keys to achieve the energy efficiency optimization of the wing-diesel engine-powered hybrid ship.

3. The energy consumption model of wing-diesel engine-powered hybrid ships

For the diesel engine-powered ship, only the main engine is adopted to provide power to overcome the sailing resistance [33]. As for the wing-diesel engine-powered hybrid ship, coupled power is provided to the ship by the diesel engine and the installed wings collaboratively. The energy consumption modeling processes of the wing-diesel engine-powered hybrid ship based on the energy transferring relationship are shown in Fig. 2.

The original energy transferring relationship among the ship-engine-propeller has been changed due to the adoption of wings.

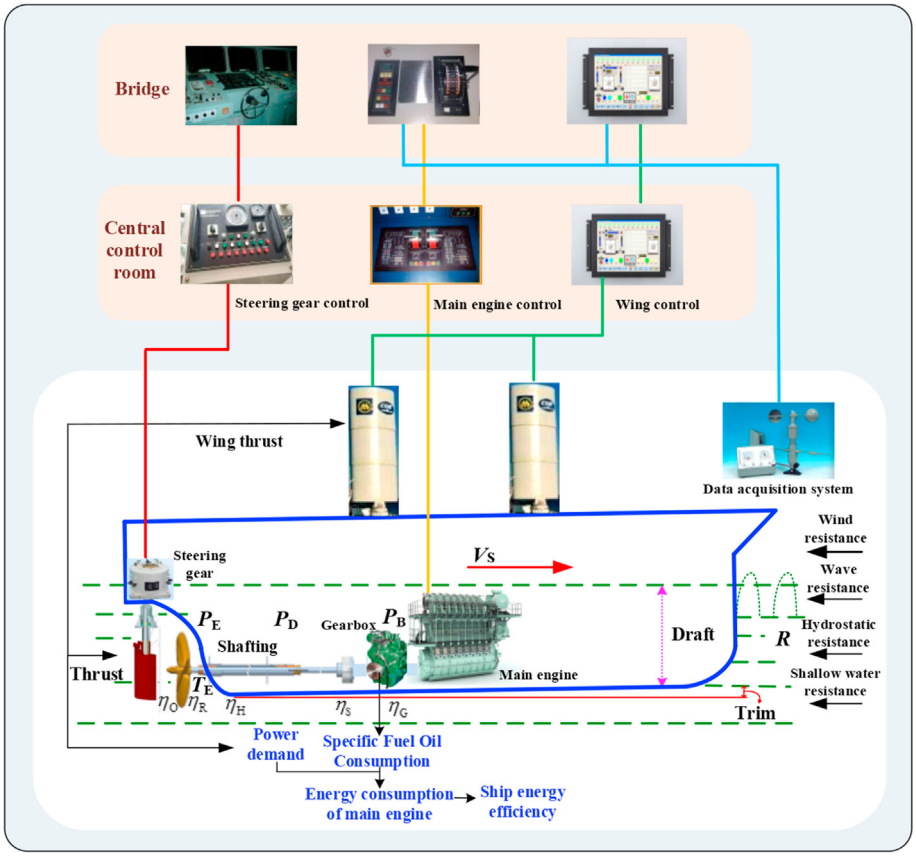

Fig. 1. Schematic diagram of the wing-diesel engine-powered hybrid power system.

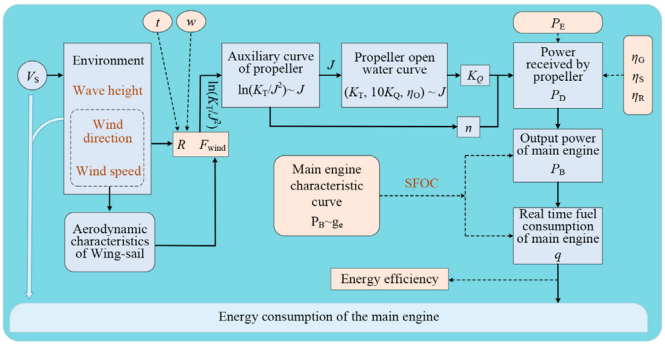

Fig. 2. Schematic diagram of the energy consumption modeling processes.

Therefore, the analysis of the new energy transferring relationship among the ship-engine-propeller-wings is important. The relationship between the sailing resistance and thrust of the ship is shown in **Eq. (1)**.

$$R = T_{\text{eff}} + T_{\text{wind}} \tag{1}$$

where, R is the total sailing resistance of the ship, N; T_{eff} is the effective thrust of the propeller, N; T_{wind} is the driving force of the wings, N.

As it can be seen from **Eq. (1)**, the propeller and the wings collaboratively provide thrust to overcome the sailing resistance of the ship and, thus, there is a coupling relationship between these two kinds of power sources. At a given speed, the thrust provided by the main engine will be reduced when the auxiliary driving force provided by the wings is increased, thereby reducing the output power and energy consumption of the main engine. Therefore, for a specific sailing speed, the thrust of the propeller can be obtained by **Eq. (2)**.

$$T_{\text{prop}} = \frac{T_{\text{eff}}}{(1-t)\cdot k} = \frac{R - T_{\text{wind}}}{(1-t)\cdot k} \tag{2}$$

where, T_{prop} is the propeller's thrust, N; t is the thrust deduction coefficient; k is the number of propellers.

The total ship resistance mainly includes the still water resistance, air resistance and wave resistance. Among them, the static water resistance of the ship can be calculated by the classical Holtrop-Mennen method, as shown in **Eq. (3)** [34].

$$R_T = R_F(1+k_1) + R_{APP} + R_W + R_B + R_{TR} + R_A \tag{3}$$

where, R_T represents the total resistance in still water, N; R_F represents the friction resistance, N; R_{APP} represents the appendages' resistance, N; R_W represents the wave making and breaking resistance, N; R_B represents the additional resistance in bulbous bow, N; R_{TR} represents the additional resistance in stern immersion, N; R_A represents the relevant resistance in model ship, N; k_1 represents the viscous resistance factor.

In addition, the air resistance that mainly indicates the wind resistance above the waterline of the ship can be obtained by **Eq. (4)** [35].

$$R_{\text{wind}} = C_A \cdot \frac{1}{2} \cdot \rho_a V_r^2 A_v \tag{4}$$

where, C_A is the wind resistance coefficient; ρ_a is the density of the air, kg/m^3; A_v is the wind resistance area of the ship, m^2; V_r is the wind speed to the ship, m/s.

Moreover, the method proposed by the International Towing Tank Conference (ITTC) is adopted to obtain the wave added resistance, as shown in **Eq. (5)** [36].

$$R_{\text{wave}} = 0.64\zeta_A^2 \cdot B^2 \cdot C_b \cdot \rho \cdot g / L \tag{5}$$

where, ζ_A is the characteristic wave height, m; B is the width of the ship, m; C_b is the square coefficient; ρ means the density of the sea water, kg/m^3; L is the length of the ship, m.

Above all, the adopted methods and algorithms for the still water resistance, wind resistance and wave added resistance had been analyzed and verified in previous published studies [34–36]. On these bases, the total resistance of the ship can be expressed by **Eq. (6)**.

$$R = R_T + R_{\text{wind}} + R_{\text{wave}} \tag{6}$$

The analysis of thrust generated by the wings is schematically shown in Fig. 3. In this figure, v_a denotes the relative wind speed (m/s), θ denotes the relative wind angle (°), and α denotes the wing attack angle (°). The force exerted on the wing can be decomposed into the lift force (F_L) in the direction that is perpendicular to the relative wind direction, and the resistance force (F_D) along the relative wind direction. The corresponding lift coefficient and resistance coefficient are C_L and C_D, respectively. F_X is the auxiliary driving force of the wing along the ship's sailing direction (N); F_Y is the side thrust of the wing in the lateral direction of the ship (N).

In addition, the schematic diagram for the analysis of the auxiliary driving force coefficient (C_X) and the lateral force coefficient (C_Y) of the wing is illustrated in Fig. 4. The coefficient C_X and C_Y can be obtained from the wing model tunnel test. As it can be seen from Fig. 4, when the wing attack angle is α_1, the wing angle is perpendicular to the ship's sailing direction and tangent to the C_L-C_D curve. In this case, the auxiliary driving force coefficient (C_{X1}) of the wing is greater than that under other wing attack angles. Therefore, at this wing attack angle, the wind energy can be effectively used to provide auxiliary power for the ship navigation.

The lift coefficient and resistance coefficient of the wing change with its attack angle. Through the synthesis and decomposition of lift and resistance force, the auxiliary driving force of the wings in the sailing direction of the ship and the side thrust of the wing in

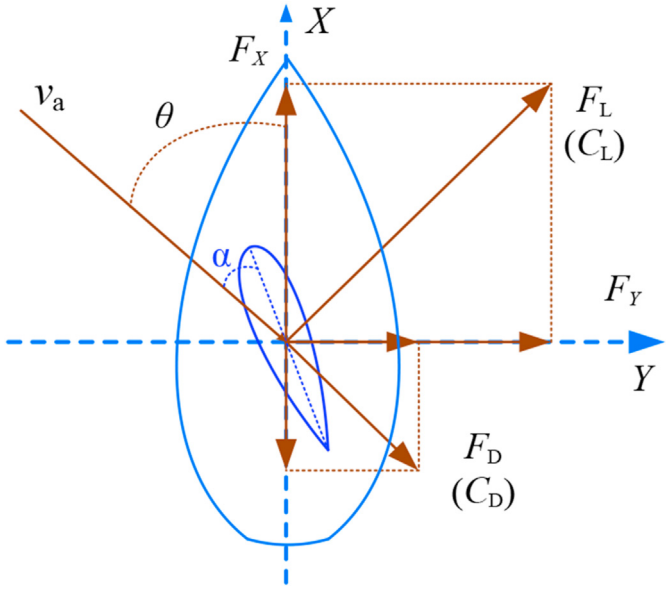

Fig. 3. Diagram of the wing force analysis.

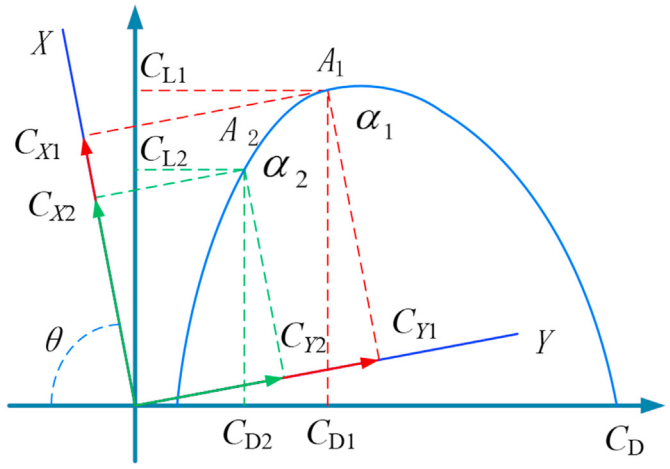

Fig. 4. The diagram for the analysis of C_L and C_D.

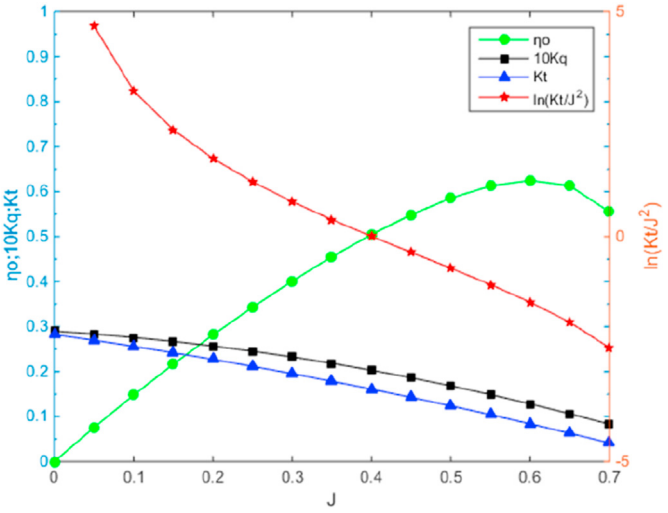

Fig. 5. The propeller open-water characteristic curve.

the lateral direction of the ship can be obtained, as shown in **Eq. (7)** and **Eq. (8)** respectively [10].

$$F_X = F_L \sin\theta - F_D \cos\theta \tag{7}$$

$$F_Y = F_L \cos\theta + F_D \sin\theta \tag{8}$$

where, the F_L and F_D can be obtained by **Eqs. (9)** and **(10)**, respectively.

$$F_L = C_L \cdot 1 \Big/ 2\rho_a {v_a}^2 \cdot S_w \tag{9}$$

$$F_D = C_D \cdot 1 \Big/ 2\rho_a {v_a}^2 \cdot S_w \tag{10}$$

where, v_a denotes the relative wind speed, m/s; S_w is the projection area of the wing, m^2.

When calculating the output power of the main engine, the auxiliary driving force of the wing along the ship's sailing direction directly offsets part of the ship's sailing resistance. In this regard, the output power of the main diesel engine can be expressed as **Eq. (11)**.

$$P_B = \frac{\left(R_{\text{ship}} - N_k \cdot F_X\right) \cdot V_s}{k \cdot \eta_S \cdot \eta_G \cdot \eta_O \cdot \eta_H \cdot \eta_R} \tag{11}$$

where, N_k indicates the number of the installed wings; V_s indicates the sailing speed of the ship, m/s; η_S indicates the shaft transmission efficiency; η_G indicates the transmission efficiency of the gearbox; η_R indicates the relative rotation efficiency of the propeller; η_H and η_O indicate the hull efficiency and the open water efficiency of the propeller respectively, which can be obtained through **Eq. (12)** and **Eq. (13)** respectively [37].

$$\eta_H = (1-t)/(1-w) \tag{12}$$

$$\eta_O = (K_T \cdot J)/(K_Q \cdot 2\pi) \tag{13}$$

where, w is the wake coefficient; J is the propeller speed coefficient, which can be obtained by **Eq. (14)**.

$$J = \frac{V_s \times (1-w)}{n \times D} \tag{14}$$

where, n is the speed of the propeller, r/s; D is the diameter of the propeller, m.

In addition, K_T and K_Q represent the propeller thrust coefficient and torque coefficient respectively, which can be expressed by **Eqs. (15)** and **(16)**, and the characteristic curve obtained from the design manual is shown in Fig. 5 [32].

$$K_T = f_{K_T}(J) \tag{15}$$

$$K_Q = f_{K_Q}(J) \tag{16}$$

Then, the fuel consumption of the main diesel engine per unit of sailing distance of the ship can be achieved by **Eq. (17)**.

$$Q_B = \frac{P_B \cdot g_e}{V_S} = f_Q(\alpha,\ V_S,\ v_a,\ \zeta_A) \tag{17}$$

where, g_e is the specific fuel oil consumption of the marine diesel engine, g/(kW·h), which is closely related to the engine power; $f_Q()$ denotes the function for calculating the energy consumption per unit of sailing distance of the ship within the segment. It is related to the wing attack angle, sailing speed of the ship, relative wind speed, and the wave height. The characteristic curve of the specific fuel oil consumption obtained from the design manual provided by the Ship Design Institute is shown in Fig. 6, which illustrates the g_e of the main diesel engine under different operational loads [32].

4. The joint optimization method of wing attack angles and sailing speeds

4.1. The joint optimization processes of wing attack angles and sailing speeds

The proposed joint optimization processes of the wing attack angles and sailing speeds are shown in Fig. 7. It mainly includes the following processes:

1) Firstly, the wind speed and wind direction are obtained from the European Centre for Medium-Range Weather Forecasts (www.ecmwf.int), and the data on ship energy efficiency are acquired by the onboard energy efficiency management system;
2) The wind information within the navigational area is analyzed to obtain the wind energy resources distribution characteristics;

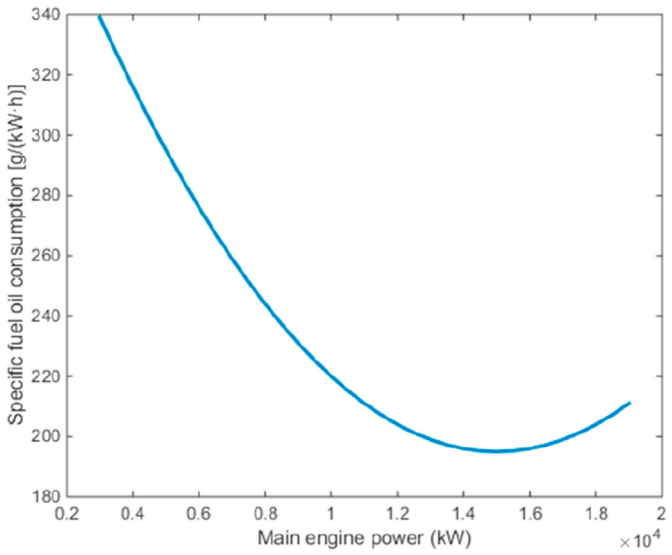

Fig. 6. The SFOC curve of the main engine.

3) The route division is conducted by adopting the *k*-means algorithm based on the distribution characteristics of the wind energy resources;
4) The joint optimization model of the wing attack angle and sailing speed is established in order to determine the optimal wing attack angles and sailing speeds that correspond to the largest auxiliary driving force of the wings and thus the minimum fuel consumption and pollution gas emissions;
5) Finally, a case study is carried out to identify the effectiveness of the proposed joint optimization method, and the energy efficiency optimization results analysis is conducted.

4.2. The joint optimization model and solution algorithm

Through the established energy consumption model of the wing-diesel engine-powered hybrid ship, the real-time fuel consumption corresponding to different sailing speeds and wing attack angles can be obtained. In this paper, the total energy consumption along a voyage is taken as the objective function, and the sailing time is taken as the main constraint, and the segment-dependent sailing speeds and wing attack angles are taken as the optimization variables. Therefore, the established non-linear optimization model of fuel consumption can be shown as follows:

$$\min Q_{total} = \sum_{i=1}^{M} \left(\left(f_Q \left(\alpha_i,\ V_{S,i},\ v_{a,i},\ \zeta_{A,i} \right) \right) \cdot S_i \right) \tag{18}$$

Subject to the following constraints:

$$T_{total} = \sum_{i=1}^{M} \left(S_i / V_{S,i} \right) \le T_{\text{limit}},\ \forall\ i \in (1,\ldots,\ M) \tag{19}$$

$$N_{\min} < n_i < N_{\max},\ \forall\ i \in (1,\ldots,\ M) \tag{20}$$

$$V_{\min} < V_{S,i} < V_{\max},\ \forall\ i \in (1,\ldots,\ M) \tag{21}$$

$$\alpha_{\min} < \alpha_i < \alpha_{\max},\ \forall\ i \in (1,\ldots,\ M) \tag{22}$$

where, M denotes the number of segments; i denotes the i^{th} segment; n is the diesel engine speed, r/min; S denotes the sailing distance, m; T_{limit} denotes the required sailing time, h.

Eq. (18) is the objective function, and the sailing speeds within different segments and the wing attack angles are the optimization variables. The first constraint in **Eq. (19)** ensures that the ship can finish a voyage within the scheduled time. The second and third ones in **Eq. (20)** and **(21)** are the physical limitations corresponding to the engine speed and the sailing speed respectively, which can avoid overload. The last one in **Eq. (22)** is the limitation

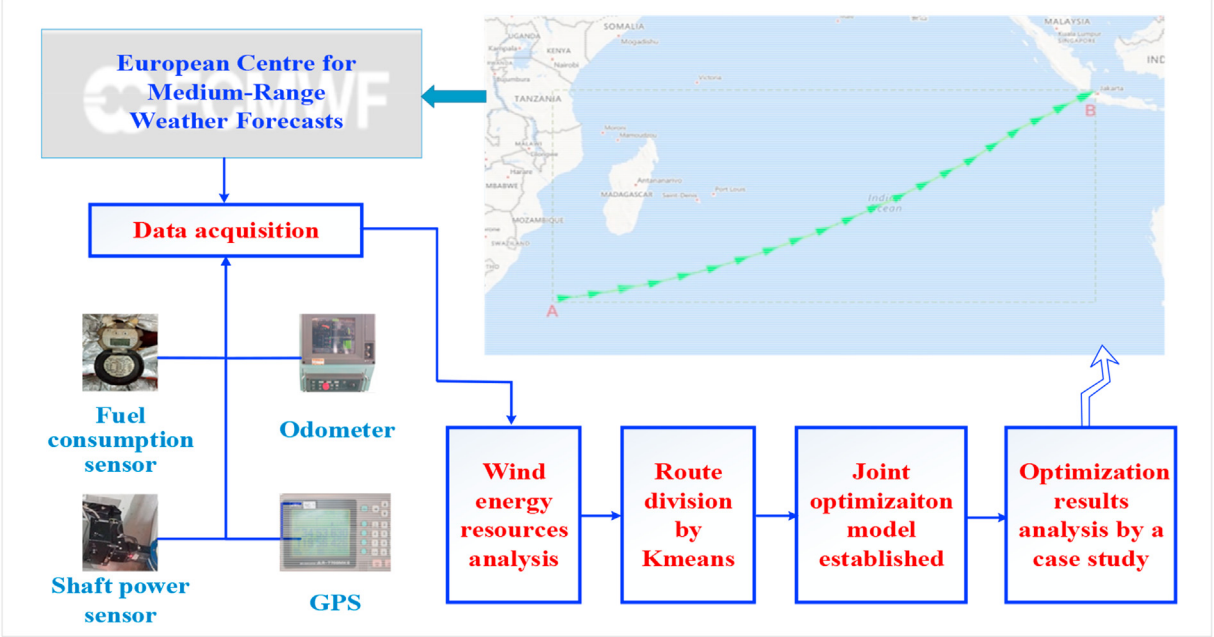

Fig. 7. The joint optimization processes of the wing attack angles and sailing speeds.

corresponding to the wing attack angle.

Particle Swarm Optimization (PSO) algorithm is a swarm intelligence algorithm. It is suitable for dealing with non-linear optimization problems and can obtain satisfactory optimization results [38]. Therefore, the PSO algorithm is adopted to solve the non-linear optimization problem concerning the optimal wing attack angles and sailing speeds under different navigational environmental conditions. The workflow is outlined as follows.

Step 1: Initialize N particles with M dimensions representing the sailing speeds corresponding to the divided route segments, and calculate the fitness value (representing the total fuel consumption along a voyage) of each particle by **Eq. (18)**, and then obtain the individual optimal value and group optimal value by comparing these fitness values.

Step 2: Update the velocity and location of each particle. The velocity and location of each particle are updated by **Eqs. (23)** and **(24)** [38].

$$V^{k+1} = w \cdot V^k + c_1 \cdot r_1 \left({p_{\text{best}}}^k - X^k \right) + c_2 \cdot r_2 \left({g_{\text{best}}}^k - X^k \right) \tag{23}$$

$$X^{k+1} = X^k + V^{k+1} \tag{24}$$

where, k denotes the number of the current iteration; P_{best} denotes the previous optimal value; g_{best} denotes the global optimal value; X denotes the particle's location; V denotes the particle's velocity; c_1 and c_2 denote the learning factors; r_1 and r_2 are random numbers; and w is the inertia weight, which can be expressed by **Eq. (25)**.

$$w = w_{max} - (w_{max} - w_{\min}) \cdot iter_{\text{current}} / iter_{\max} \tag{25}$$

where, $w_{\max}$ denotes the maximum inertia factor; $w_{\min}$ denotes the minimum inertia factor; $iter_{\text{current}}$ denotes the current iteration number; and $iter_{\max}$ denotes the maximum iteration number.

Step 3: Recalculate the fitness value of each particle that meets the constraints in **Eqs.** (19)-(22), then update the optimal values of the individual particles and the overall population;

Step 4: Go to *Step 2* and iterative operation until the algorithm converges, then the optimized individuals (namely the optimized sailing speeds and wing attack angles) can be obtained.

5. The energy consumption optimization analysis

5.1. The introduction of the research target

Considering the operational characteristics of the rigid-wing sail and its reliability, the ship adopting the wing-diesel engine-powered hybrid power system should have the characteristics of wide shape, small size of superstructure and suitable main deck for the wings' installation and operation. In these regards, the bulk carriers and oil tankers have natural advantages and the superior conditions for installing the wing-diesel engine-powered hybrid power system. Therefore, a 300,000 DWT VLOC is selected as the research target in this paper. The basic parameters of the ship are shown in Table 1 [39].

Table 1
The main parameters of the target ship.

Item	Parameter	Item	Parameter
Length	327 m	Design speed	14.5 kn
Depth	29 m	Number of propeller's blades	5
Width	55 m	Diameter of propeller	9.7 m
Deadweight	297,959 t	Engine rated power	19,000 kW
Draft	21.4 m	Engine rated speed	73 rpm

The energy consumption data acquisition scheme, as shown in Fig. 8, is adopted to collect the data including fuel consumption, power, engine speed, sailing speed, and position of the target ship. This system lays a solid foundation for the analysis of the ship's energy consumption optimization.

The Arc-shaped symmetrical rigid wings with same parameters arranged in parallel are analyzed for the target ship, by comprehensively considering the ship's size, the deck's layout and the space for installing the wings. The schematic diagram of this arrangement is shown in Fig. 9. This kind of arrangement can not only improve the utilization efficiency of wind energy, but also improve the utilization efficiency of the deck space. The specific parameters of the analyzed target wings are shown in Table 2.

5.2. The analysis of the wing's aerodynamic characteristics

For the analysis of the force generated by the wings, the lift and resistance coefficients are important parameters for calculating the auxiliary driving force and lateral force of the wings, which can be obtained through the wind tunnel test. The wind tunnel for the test is a low-speed wind tunnel with closed single flow. The power is provided by a DC motor with 1250 kW. The wind speed for the test is 3–93 m/s and can be adjusted continuously. In addition, the mechanical balance β system is used to control the wind angle of the sail model, and the F_{D} and F_{L} were measured by a mechanical balance, as shown in Fig. 10. The wing-type model used in the tunnel test is that of the target wing scaled down by 40 times. The similarity criteria including the geometric similarity, kinematic similarity and dynamic similarity were considered for the test. Therefore, the lift and resistance coefficients of the target wing can be calculated by Eqs. (9) and (10) through measuring the corresponding lift and resistance coefficients of the wing-type model. The corresponding relationship between the lift and resistance coefficients of the wing is shown in Fig. 11.

According to the lift coefficient, resistance coefficient and the wing attack angle, the auxiliary driving force coefficient and lateral force coefficient of the wings can be calculated, as shown in **Eqs. (26)** and **(27)**, respectively.

$$C_X = C_L \sin\theta - C_D \cos\theta \tag{26}$$

$$C_Y = C_L \cos\theta + C_D \sin\theta \tag{27}$$

Then, the auxiliary driving force and the lateral force of the wings can be obtained through **Eqs. (28)** and **(29)**, respectively.

$$F_X = C_X \cdot 1 \Big/ 2\rho_a v_a^2 \cdot S_w \tag{28}$$

$$F_Y = C_Y \cdot 1 \Big/ 2\rho_a v_a^2 \cdot S_w \tag{29}$$

Finally, the auxiliary driving force coefficients of the wings under different wind angles and wing attack angles are shown in Fig. 12. In addition, the maximum auxiliary driving force coefficients of the wings at different wind angles are shown in Fig. 13.

5.3. The wind energy resources analysis and route division

The statistical analysis of the wind energy resources within the navigational area is the premise for the energy consumption optimization analysis of the wing-diesel engine-powered hybrid ship. The wind energy resources within the navigational area not only determine whether the hybrid power system can be put into use, but also influence the utilization efficiency of the wind energy and

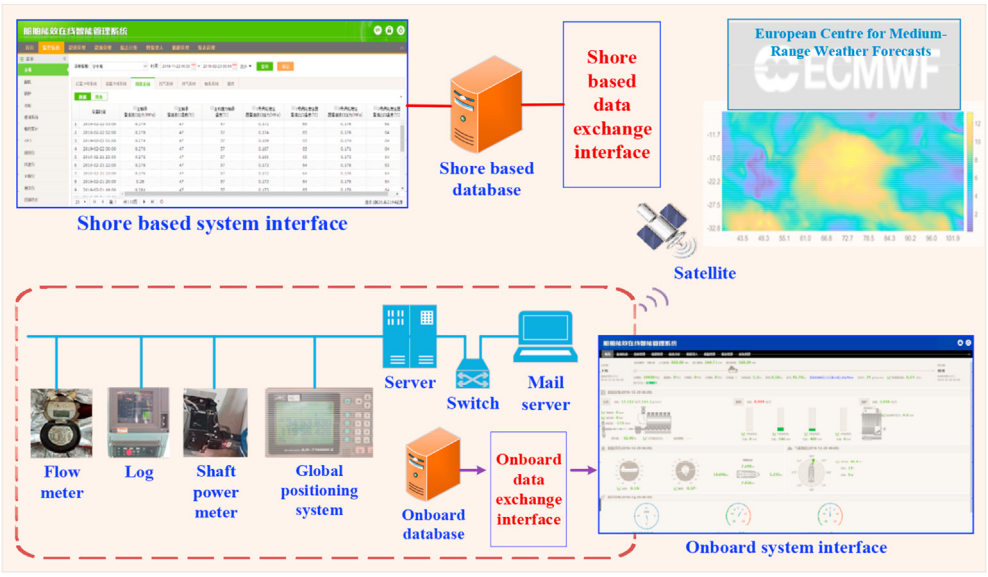

Fig. 8. The illustration of energy consumption data acquisition scheme for the target ship.

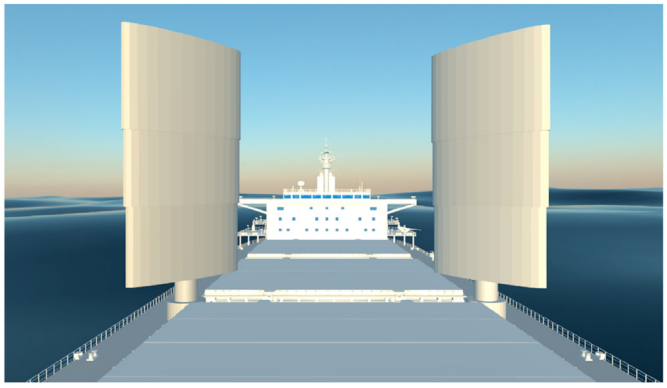

Fig. 9. The schematic diagram of the double wings arranged in parallel on the main deck.

its contribution to the optimization of ship's energy consumption. In this study, the navigational area in the India Ocean between position A (33.4046 °S, 37.7470 °E) and B (6.4954 °S, 105.0087 °E) is selected as the target area, as shown in Fig. 14. The seasonal characteristics of the wind energy resource in this navigational area are obvious. The wind energy resources in this area are stable during the same monsoon period, and thus can contribute to the practical application of the wing-diesel engine-powered hybrid power system.

The data used in this paper, including wind direction and speed as well as wave height, are obtained from the European Centre for Medium-Range Weather Forecasts (www.ecmwf.int). The minimum grid interval ($0.125° \times 0.125°$) is used for the data acquisition, in order to ensure the accuracy of the obtained data. The collection frequency is once every 6 h. In addition, the obtained data is preprocessed including: 1) the real-time dynamic data of the navigational environment at different positions and different time is obtained by three-dimensional linear interpolation method; 2) the wind field components in the latitude and longitude direction are vector synthesized to obtain the final data of the wind speed and direction. The obtained data of the wind speed and direction at different longitudes and latitudes at a certain time (2015-06-26 18:00) is partly shown in Table 3 and Table 4, respectively.

Based on the obtained data, the spatial and temporal distribution analysis of the wind speed and direction within the navigational area is carried out. It lays a foundation for analyzing the distribution of wind energy resources and their contribution to the energy consumption optimization of the wing-diesel engine-powered hybrid ship. The spatial and temporal distribution of the wind speed and wind direction within this area is partly shown in Fig. 15 and Fig. 16, respectively.

In addition, the analysis of the distribution characteristics of the wind energy resources is conducted, in order to further analyze the characteristics of the wind speed and wind direction in this area. The distribution characteristics of the wind energy resources are shown by the wind rose diagrams in Fig. 17. The wind rose diagram is one kind of professional statistical charts that can be used for quantitative analysis of the wind components. It can be used to show the frequency of wind direction and speed in a period of time within a certain area, which is important to reflect the characteristics of regional wind energy resources. As it can be seen from Fig. 17, the wind direction is basically concentrated between about 270° and 345°, and the wind speed is mainly concentrated between about 6 m/s and 12 m/s for the given time. It can be concluded that the relatively stable wind direction and speed in this navigational area could provide favorable conditions for the application of the wing-diesel engine-powered hybrid power system.

According to the analysis results of the wind energy resources

Table 2
The parameters of the analyzed rigid-wing sail.

The wing height/(m)	The wing projected area/(m^2)	The wing chord length/(m)	The aspect ratio /dimensionless
40	960	24	1.67

Fig. 10. The diagram of the wind tunnel experiment.

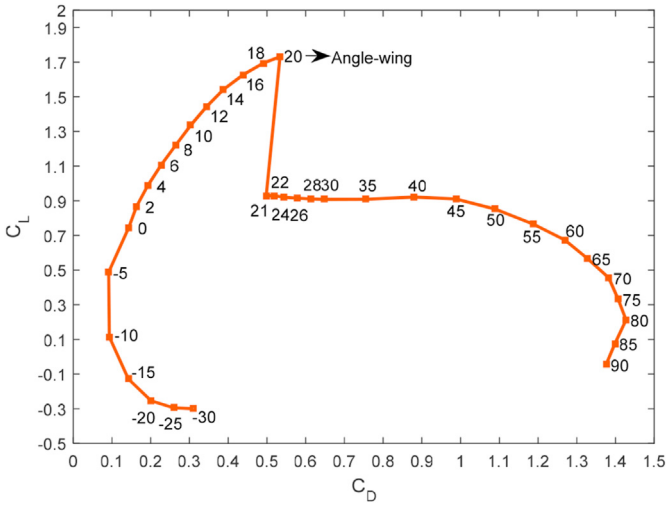

Fig. 11. The C_L-C_D curve of the wing.

within the target navigational area, the wind energy resources in different positions within the typical routes exhibit obvious differences. Therefore, the route division is important to achieve the fuel consumption optimization under different environmental conditions. The clustering algorithm can be adopted to realize the route division based on the analysis of environmental conditions. The *k*-means clustering algorithm is a type of clustering analysis based on the similarity theory. By adopting the *k*-means algorithm, the position with the same characteristics of environmental conditions would be clustered to a segment [40]. The clustering results can be used as the basis for the route division. Then, the joint optimization of the wing attack angle and the sailing speed based on the route division can be realized. Through this way, the

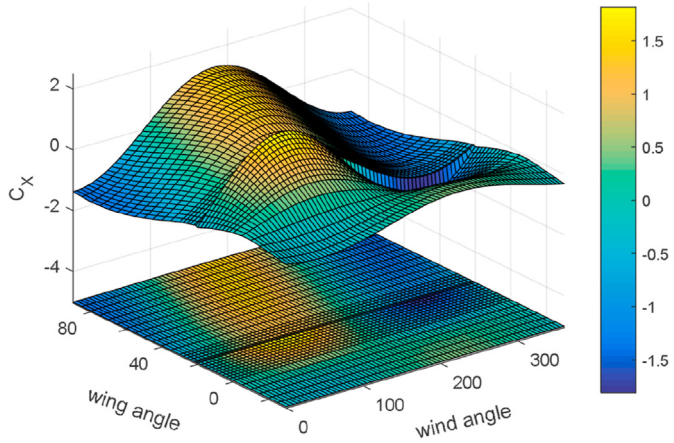

Fig. 12. The auxiliary driving force coefficients of the wing under different conditions.

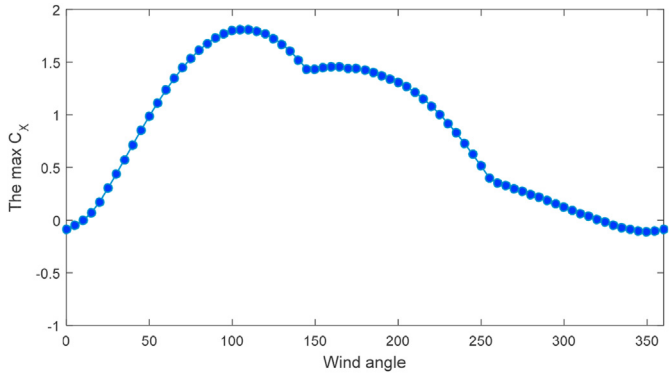

Fig. 13. The maximum auxiliary driving force coefficients of the wing under different conditions.

frequent adjustment of the wing attack angle and main engine speed can be avoided. This is conducive to the practical application of the joint optimization method. The division results of the target route based on clustering algorithm and the environmental conditions are shown in Fig. 18. As it can be seen, the whole route can be divided into 14 segments according to the characteristics of environmental conditions, and the wind energy resources of which are different in each segment.

5.4. The numerical analysis of energy consumption optimization and discussions

A typical voyage is taken as an example to analyze the energy consumption and CO_2 emissions when the ship would adopt the wing-diesel engine-powered hybrid power system and the proposed joint optimization method. The navigational information is partly shown in Table 5.

Based on the established energy consumption model and the statistical analysis results of the wind energy resources, the optimal sailing speeds and wing attack angles can be obtained through the proposed joint optimization algorithm under different wind conditions and operational conditions. The related parameters required by the PSO algorithm are shown in Table 6. The optimal sailing speeds in each divided segment and the wing attack angles along the route are shown in Fig. 19 and Fig. 20, respectively.

The auxiliary driving force coefficients under the optimal wing attack angles are shown in Fig. 21. In addition, the energy

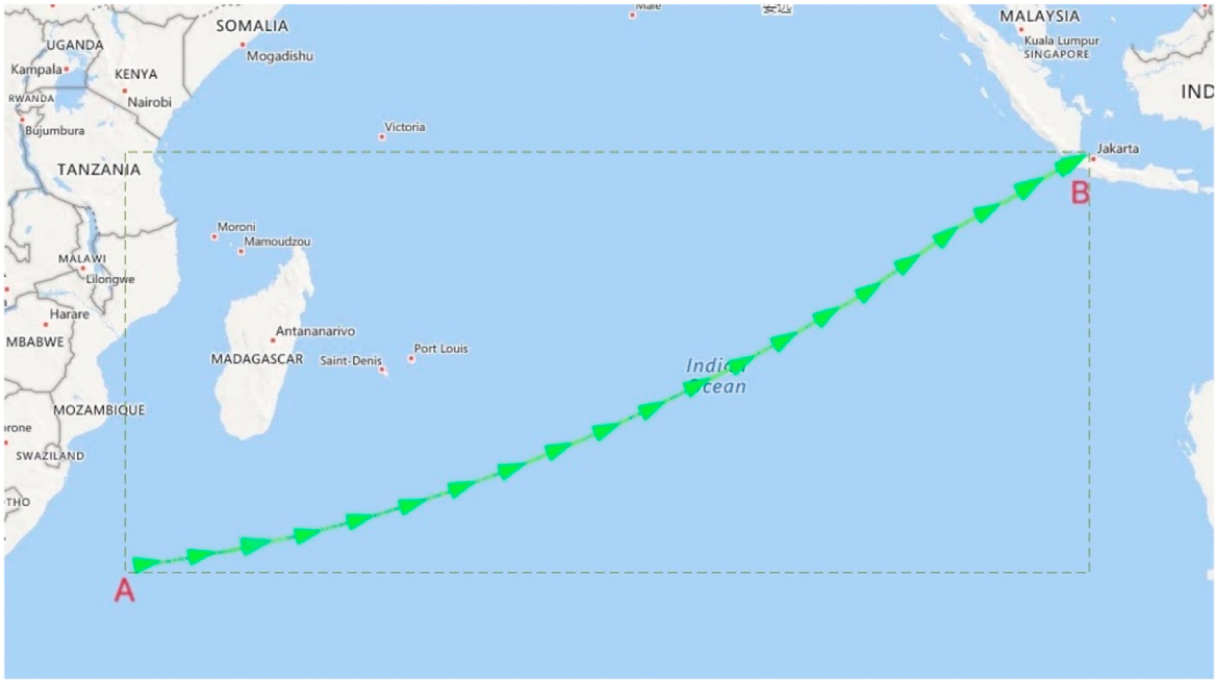

Fig. 14. The schematic diagram of the navigational area and the sailing route.

Table 3
The wind speed at different longitudes and latitudes (2015-06-26 18:00).

Latitude /(°)	Longitude/(°)							
	37.625	37.750	37.875	38.000	…	104.750	104.875	105
−6.375	2.677	2.709	2.832	2.906	…	2.738	2.430	2.192
−6.500	2.820	2.727	2.758	2.829	…	2.830	2.522	2.289
−6.625	2.963	2.870	2.777	2.759	…	2.948	2.643	2.417
−6.750	2.991	2.898	2.806	2.786	…	3.259	2.956	2.735
−6.875	2.967	2.875	2.879	2.881	…	3.660	3.358	3.138
−7.000	2.953	2.942	2.968	2.983	…	4.062	3.762	3.543
…	…	…	…	…	…	…	…	…
−33.125	4.564	4.628	4.692	4.756		2.810	2.810	2.823
−33.250	4.544	4.607	4.669	4.732		2.442	2.430	2.433
−33.375	4.531	4.591	4.651	4.713		2.079	2.051	2.037
−33.500	4.527	4.585	4.644	4.702		1.737	1.683	1.644

consumption and CO_2 emissions before and after adopting the hybrid power system and the proposed joint optimization method are shown in Fig. 22 and Fig. 23, respectively. The CO_2 emissions are obtained by multiplying the fuel consumption by the CO_2 conversion rate that is 3.114 for the heavy fuel oil [41]. As it can be seen from these figures, the energy consumption of the ship can be reduced effectively in most positions by adopting the wing-diesel engine-powered hybrid power system and the joint optimization method, although the percentage reduction of the fuel consumption is different. The main reason is that the different wind angles lead to the different utilization efficiency of the wind energy. When the relative wind angle is between 0° and 40°, the optimization effect of the fuel consumption is weak due to the poor auxiliary driving force of the wings, as shown in Fig. 12. When the wind angle is nearly 90°, the auxiliary driving force of the wings is stronger, which makes the optimization effect of the energy consumption better. Similarly, the CO_2 emissions are the lowest as the wind angle approaches nearly 90°. It should be noted that the wing cannot be used when the auxiliary driving force coefficient is less than 0.

In addition, Because of the sailing time constraint, the ship has to improve the sailing speed in some positions to ensure arriving at destination on time, which lead to the increase of the energy consumption and CO_2 emissions. Although the optimal energy consumption and CO_2 emissions in some positions are higher than the original operational mode, the total energy consumption and CO_2 emissions of the ship can be reduced effectively when adopting

Table 4
The wind direction at different longitudes and latitudes (2015-06-26 18:00).

Latitude /(°)	Longitude/(°)							
	37.625	37.750	37.875	38.000	…	104.750	104.875	105.000
−6.375	318.006	319.519	321.842	323.096		278.779	278.287	278.934
−6.500	317.624	317.700	319.189	320.544		284.473	284.707	285.972
−6.625	317.286	317.357	317.432	317.846		289.769	290.580	292.353
−6.750	319.182	319.312	319.451	314.899		292.370	293.371	295.155
−6.875	322.233	322.462	316.845	311.921		293.511	294.509	296.145
−7.000	325.339	319.843	313.904	309.137		294.438	295.391	296.904
…	…	…	…	…	…	…	…	…
−33.125	356.539	356.069	355.609	355.162		253.693	256.004	258.245
−33.250	358.555	358.054	357.558	357.084		247.611	250.277	252.895
−33.375	0.884	0.343	359.823	359.316		238.826	241.865	244.955
−33.500	3.819	3.247	2.681	2.138		224.628	227.940	231.518

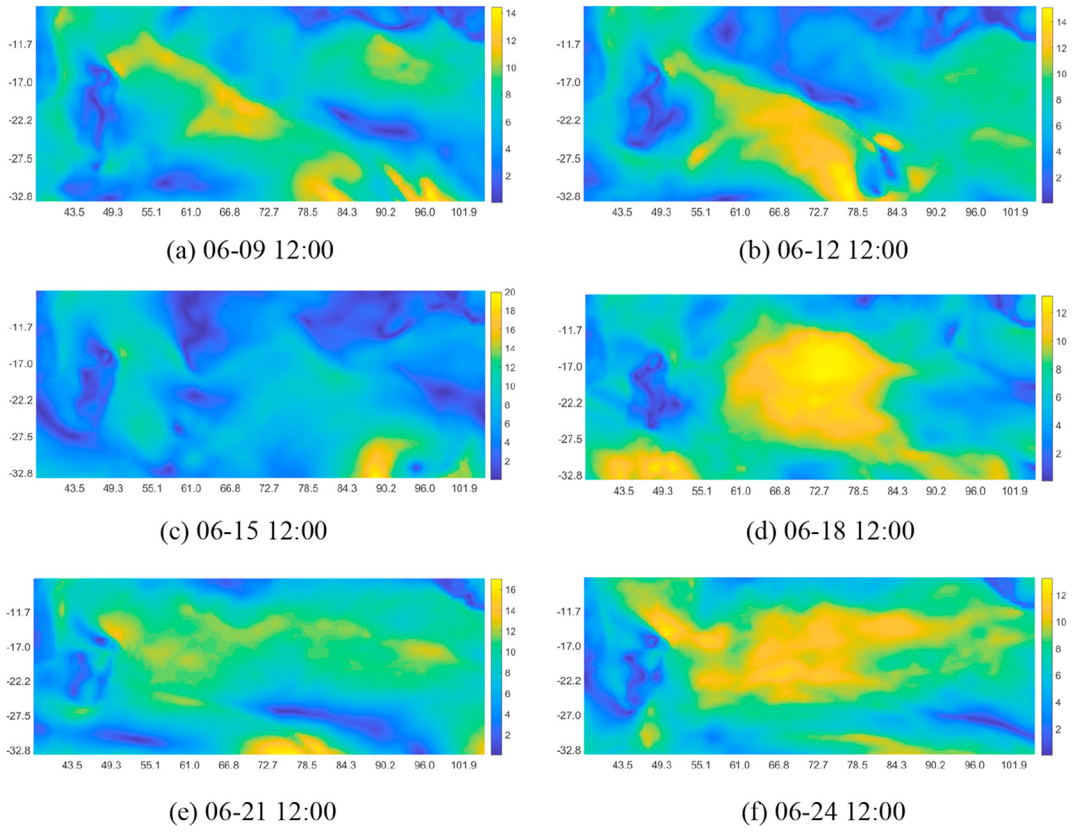

Fig. 15. The spatial and temporal distribution characteristics of the wind speed.

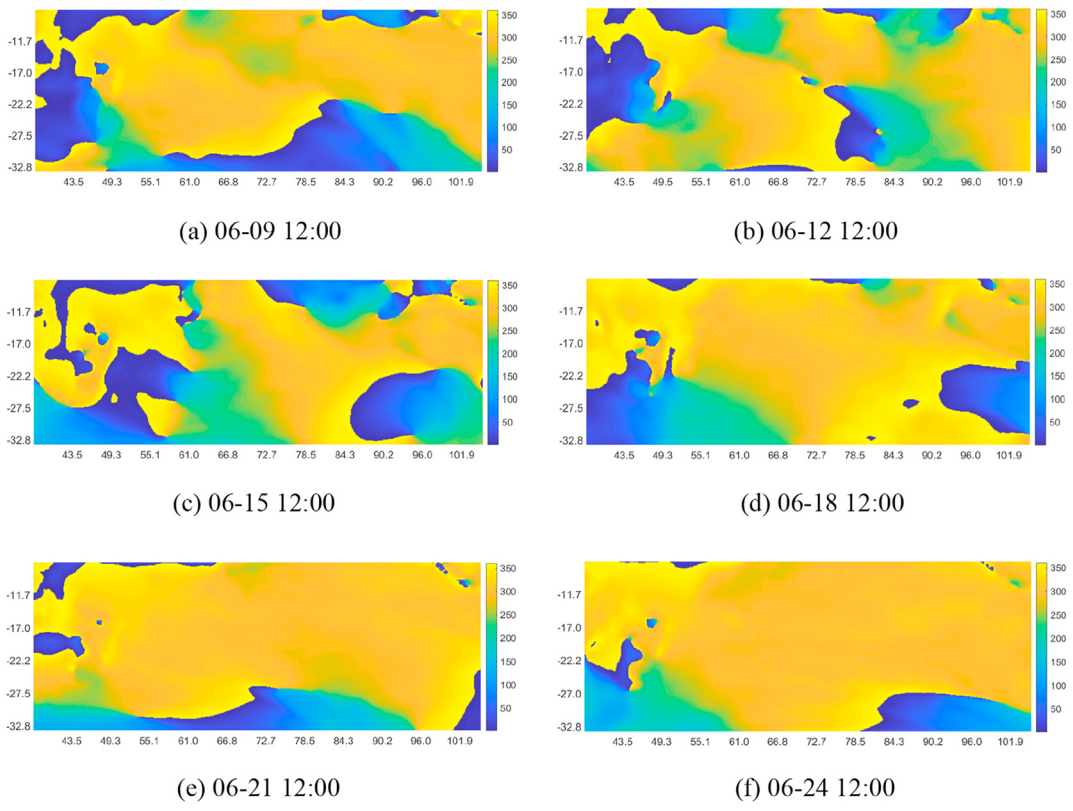

Fig. 16. The spatial and temporal distribution characteristics of the wind direction.

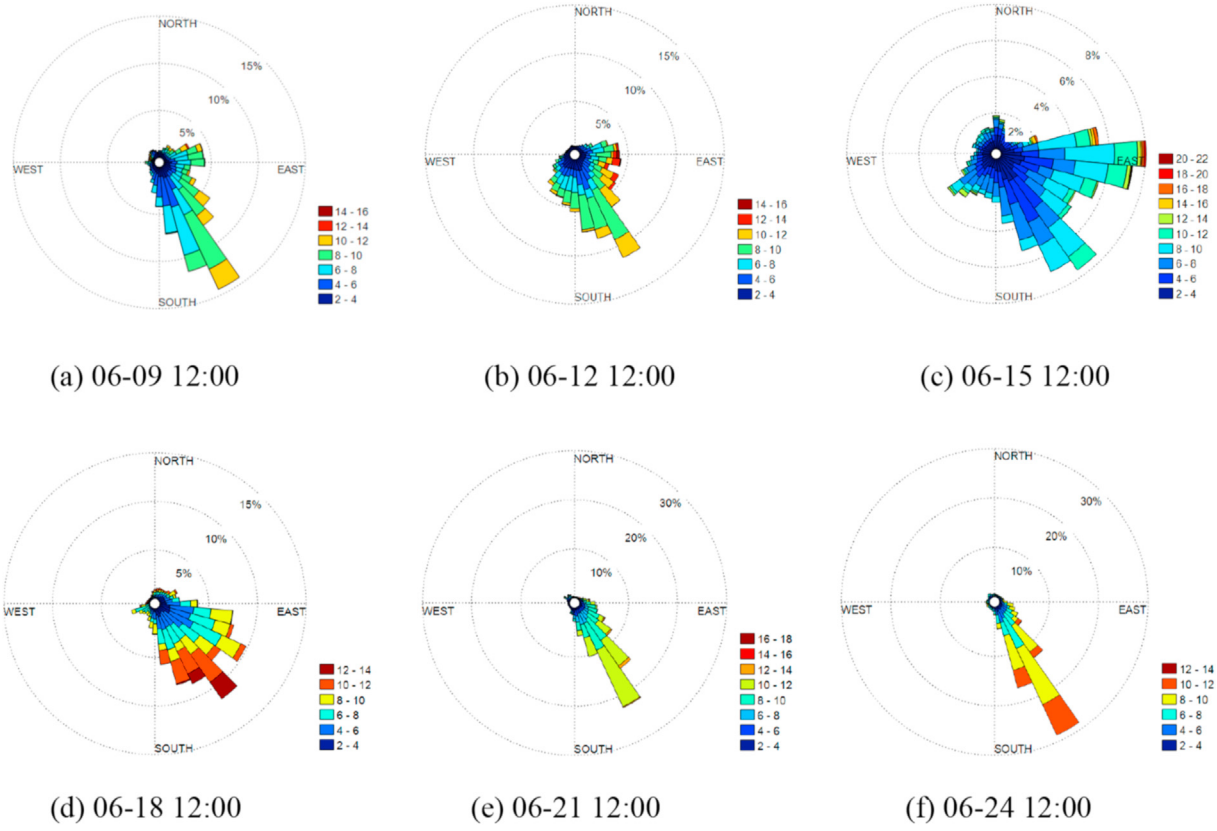

Fig. 17. The wind rose diagram within the target navigational area.

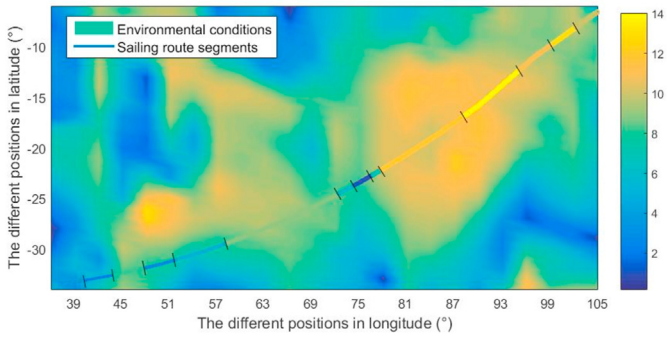

Fig. 18. The route division results based on clustering algorithm and environmental conditions.

the wing-diesel engine-powered hybrid power system and the proposed joint optimization method. The specific total energy consumption and CO_2 emissions of the ship in the whole voyage before and after adopting the wing-diesel engine-powered hybrid power system and the proposed joint optimization method are shown in Table 7. As it can be seen, the fuel consumption and CO_2 emissions can be reduced by as much as 4.5% through adopting the wing-diesel engine-powered hybrid power system and the proposed joint optimization method. This means about 40 tons of fuel can be saved after adopting the wing-diesel engine-powered hybrid power system for this single voyage, and thus about 142,000 RMB (taking the price of the heavy fuel oil as 3550 RMB per tonnage) can be saved for this voyage. Therefore, it can effectively improve the economy of the shipping company. In addition, about

Table 6
Parameters required by the joint optimization algorithm.

Parameters	c_1	c_2	w_{max}	w_{min}	$iter_{max}$	N	M
Values	2	2	0.9	0.4	50	20	14

Table 5
Part of the navigational information of the target ship.

Data sequence	Longitude /(°)	Latitude /(°)	Shaft power/(kW)	Sailing speed /(kn)	Fuel consumption /(kg/n mile)	Wind speed /(m/s)	Wind direction /(°)	Wave height /(m)
1	37.747 E	33.405 S	10,020	9.2	250.96	4.41	184.70	2.52
2	37.777 E	33.401 S	9950	9.2	231.07	4.36	185.65	2.52
3	37.809 E	33.398 S	9970	9.3	241.82	4.28	185.38	2.52
4	37.839 E	33.394 S	9980	9.2	257.39	4.21	185.00	2.52
5	37.869 E	33.391 S	9930	9.2	230.93	4.13	184.55	2.51
6	37.900 E	33.387 S	9790	9.4	240.32	4.06	184.06	2.51
7	37.930 E	33.384 S	9900	9.0	251.59	3.98	183.47	2.51
…	…	…	…	…	…	…	…	…

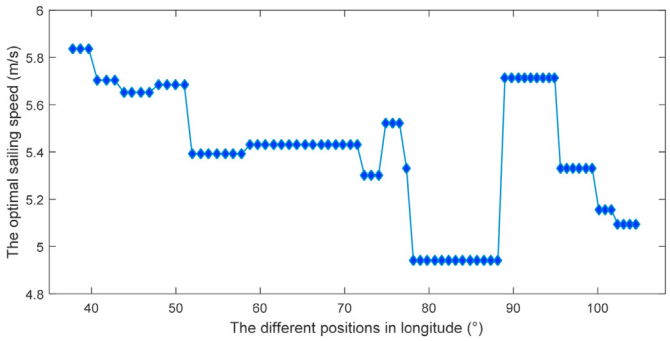

Fig. 19. The optimal sailing speeds at different sailing positions along the route.

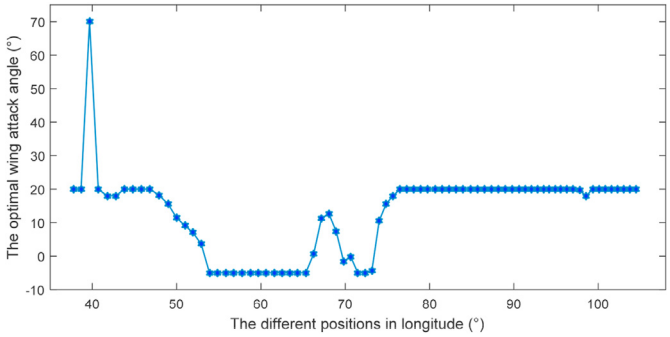

Fig. 20. The optimal wing attack angles at different sailing positions along the route.

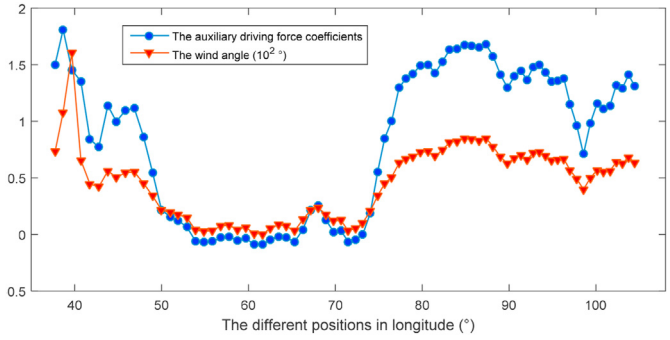

Fig. 21. The auxiliary driving force coefficients under the optimal wing attack angles.

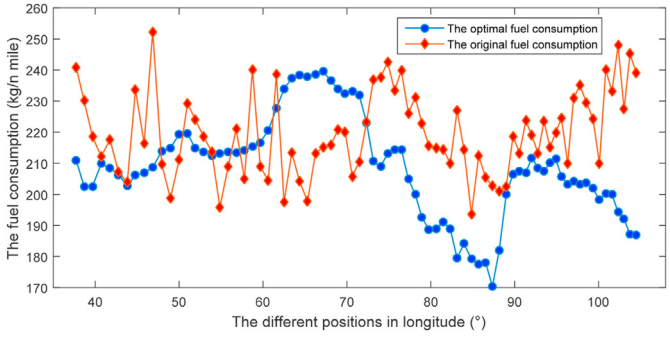

Fig. 22. Comparative analysis of the energy consumption at different sailing positions.

125 tons of CO_2 emissions can be reduced by adopting the wing-diesel engine-powered hybrid power system and the optimization method for this single voyage.

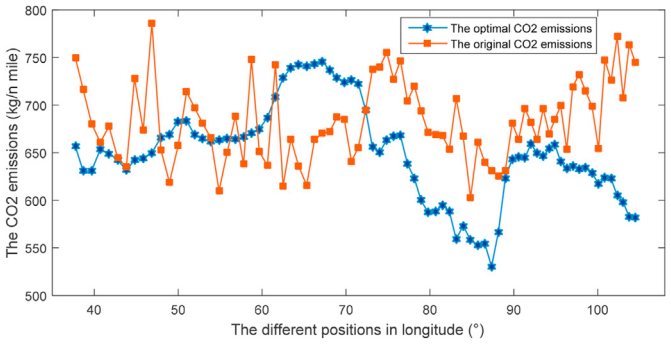

Fig. 23. Comparative analysis of the CO_2 emissions at different sailing positions.

The energy consumption model proposed in this study was established based on a theoretical analysis of the energy relationship between the power and wing systems. The effects of winds and waves on the propulsion characteristics of the propeller and on the fuel consumption characteristics of the main engine under different navigational conditions were both considered when modeling the ship energy consumption. The energy consumption model was also based on a theoretical analysis of the energy conversion. The models and algorithms adopted here for investigating the sailing resistance, the wing thrust, and the engine output power had been analyzed and verified in previous published studies. Hence, we were sure about their effectiveness and applicability in relation to the target type of ship. However, the established model ignores the impact of navigational environmental factors on the ship's sailing posture (e.g., trim and roll). In fact, when sailing in a normal navigational environment, the impact of small changes in sailing posture on the ship's energy consumption can be ignored. In addition, the influence of bottom fouling on the ship's energy consumption and changes in the power system characteristics due to equipment aging are ignored by the established model. Although these last factors have little impact on newly-built ships, the operation characteristic curve of the power system should be updated for long-time running ships. Moreover, the influence of ship bottom fouling on the ship's resistance and, thus, on energy consumption should be considered. Therefore, in the case of long-time running ships, a large number of practical operational data should be used to modify the model parameters. This would improve the model accuracy and the optimization potential of the ship energy efficiency. In this study, the target ship is relatively a new one and, thus, the influence of equipment aging and performance degradation is ignored.

In addition, from the optimization results, the application of the wing-diesel engine-powered hybrid system and the proposed optimization method can effectively realize energy saving and emission reduction in the shipping industry. Notably, the optimization level of the energy consumption and CO_2 emissions would be higher if more wings are installed (only two wings are installed for the target ship in this study) and more suitable wind energy resources are available.

6. Conclusions and the future research works

The wing-diesel engine-powered hybrid power system can effectively reduce energy consumption and pollution gas emissions by using wind energy as the auxiliary driving force. In this paper, an energy consumption model of the wing-diesel engine-powered hybrid ship is established based on the energy transfer analysis of the wing-diesel engine-powered hybrid power system. The model

Table 7
Comparative analysis of energy consumption and CO_2 emissions of the whole voyage.

Items	Wing installed	Wing uninstalled	Optimized percent
Total fuel consumption (t)	845.25	884.97	4.5%
Total CO_2 emissions (t)	2632.1	2755.8	4.5%

can effectively describe the energy consumption of the wing-diesel engine-powered hybrid ship under different sailing speeds and wing attack angles. In addition, a joint optimization method of the wing attack angle and sailing speed for the wing-diesel engine-powered hybrid ship was proposed by adopting the PSO algorithm, in order to reduce fuel consumption and CO_2 emissions of the ship under different navigational environmental conditions. The study results show that the energy consumption and CO_2 emissions can be reduced by as much as about 4.5% of the target ship by adopting the wing-diesel engine-powered hybrid power system and the proposed joint optimization method. The optimization potential of the energy consumption would be much higher if more wings are installed and more suitable wind energy resources are available. Therefore, the proposed method can provide references for the practical operation and management of the wing-diesel engine-powered hybrid ships.

We further analyzed the optimization potential of energy consumption by adopting a wing-diesel engine-powered hybrid power system and optimizing it. Notably, the energy efficiency of the hybrid power ship is not only related to the operational status of the wings and of the sailing speeds, but also to the sailing route and the sailing status of the ship. Therefore, the optimization potential of the ship energy efficiency can be further enhanced through a comprehensive optimization control of the sailing route, of the sailing speeds, of the wing attack angles, and of the sailing status. In order to maximize the ship energy efficiency, future research should hence focus on the development of a comprehensive optimization model and of a control algorithm of the sailing route, sailing speeds, wing attack angles, and sailing status.

Credit author statement

Kai Wang: Conceptualization, methodology, software, validation, investigation, resources, writing-original draft preparation, funding acquisition; **Yu Xue:** validation, formal analysis, investigation; **Hao Xu:** software, data curation, writing-original draft preparation; **Lianzhong Huang:** Conceptualization, resources, writing-review and editing, supervision, project administration, funding acquisition; **Ranqi Ma:** Methodology, validation, writing-original draft preparation, visualization; **Peng Zhang:** formal analysis; **Xiaoli Jiang:** writing-review and editing, visualization; **Yupeng Yuan:** data curation; **Rudy R. Negenborn:** supervision; **Peiting Sun:** supervision, project administration.

Declaration of competing interest

The authors declare that they have no known competing financial interests or personal relationships that could have appeared to influence the work reported in this paper.

Acknowledgements

The authors are grateful to the support of the National Natural Science Foundation of China (51909020, 52071045), the Project Funded by China Postdoctoral Science Foundation (2020M670735, 2021T140080), the Project from Key Lab. of Marine Power Engineering and Tech. authorized by MOT (KLMPET2020-06), and the Fundamental Research Funds for the Central Universities (3132019316).

References

[1] Wang K, Yan X, Yuan Y, Li F. Real-time optimization of ship energy consumption based on the prediction technology of working condition. Transport Res Transport Environ 2016;4:81–93.
[2] Chi H, Pedrielli G, Ng SH, Kister T, Bressan S. A framework for real-time monitoring of energy efficiency of marine vessels. Energy 2018;145:246–60.
[3] Marine Environment Protection Committee (MEPC). Prevention of air pollution from ships (Third IMO GHG Study 2014). London: Marine Environment Protection Committee; 2014.
[4] Xing H, Spence S, Chen H. A comprehensive review on countermeasures for CO_2 emissions from ships. Renew Sustain Energy Rev 2020;134:110222.
[5] Yuan Y, Wang J, Yan X, Li Q, Long T. A design and experimental investigation of a large-scale solar energy/diesel generator powered hybrid ship. Energy 2018;165:965–78.
[6] Jafarzadeh S, Utne IB. A framework to bridge the energy efficiency gap in shipping. Energy 2014;69:603–12.
[7] Silva MF, Friebe A, Malheiro B, Guedes P, Ferreira P, Waller M. Rigid wing sailboats: a state of the art survey. Ocean Eng 2019;187:1–20.
[8] Ballini F, Ölçer AI, Brandt J, Neumann D. Health costs and economic impact of wind assisted ship propulsion. Ocean Eng 2017;146:477–85.
[9] Li CL, Zhou S, Han Y. Research on the influence of wind energy on new energy utilization coefficient of EEDI. Adv Mater Res 2013;744:561–5.
[10] Ma Y, Bi H, Hu M, Zheng Y, Gan L. Hard sail optimization and energy efficiency enhancement for sail-assisted vessel. Ocean Eng 2019;173:687–99.
[11] Persson A, Lindstrand R, Muggiasca S, Larsson L. CFD prediction of steady and unsteady upwind sail aerodynamics. Ocean Eng 2017;141:543–54.
[12] Augier B, Bot P, Hauville F, Durand M. Dynamic behaviour of a flexible yacht sail plan. Ocean Eng 2013;66:32–43.
[13] Lee H, Jo Y, Lee D, Choi S. Surrogate model based design optimization of multiple wing sails considering flow interaction effect. Ocean Eng 2016;121:422–36.
[14] Li Q, Nihei Y, Nakashima T, Ikeda Y. A study on the performance of cascade hard sails and sail-equipped vessels. Ocean Eng 2015;98:23–31.
[15] He J, Hu Y, Tang JJ, Xue S. Research on sail aerodynamics performance and sail-assisted ship stability. J Wind Eng Ind Aerod 2015;146:81–9.
[16] Viola IM, Sacher M, Xu JS, Wang F. A numerical method for the design of ships with wind-assisted propulsion. Ocean Eng 2015;105:33–42.
[17] Wang K, Li JY, Huang LZ. A novel method for joint optimization of the sailing route and speed considering multiple environmental factors for more energy efficient shipping. Ocean Eng 2020;216:107591.
[18] Simić A, Radojčić D. On energy efficiency of inland waterway self-propelled cargo vessels. FME Trans 2013;41:138–45.
[19] Bondarenko O, Fukuda T. Development of a diesel engine's digital twin for predicting propulsion system dynamics. Energy 2020;196:117126.
[20] Lu R, Turan O, Boulougouris E, Banks C, Incecik A. A semi-empirical ship operational performance prediction model for voyage optimization towards energy efficient shipping. Ocean Eng 2015;110:18–28.
[21] Wang S, Shen X, Zhao J, Ji B, Yang P. Prediction of marine meteorological effect on ship speed based on ASAE deep learning. J Traffic Transport Eng 2018;18(2):139–47.
[22] Masuyama Y, Tahara Y, Fukasawa T, Maeda N. Database of sail shapes versus sail performance and validation of numerical calculations for the upwind condition. J Mar Sci Technol 2009;14(2):137–60.
[23] Kolk NJ, Keuning JA, Huijsmans RHM. Part 1: experimental validation of a RANS-CFD methodology for the hydrodynamics of wind-assisted ships operating at leeway angles. Ocean Eng 2019;178:375–87.
[24] Deng YJ, Zhang XK, Zhang GQ. Fuzzy logic based speed optimization and path following control for sail-assisted ships. Ocean Eng 2019;171:300–10.
[25] Deng YJ, Zhang XK, Zhang Q, Hu YC. Event-triggered composite adaptive fuzzy control of sailboat with heeling constraint. Ocean Eng 2020;211:107627.
[26] Viola IM, Sacher M, Xu J, Wang F. A numerical method for the design of ships with wind-assisted propulsion. Ocean Eng 2015;105:33–42.
[27] Shtikla P, Ghosh K. Revival of the modem wing sails for the propulsion of commercial ships. World Academy of Science, Engineering and Technology; 2009. p. 398–403.
[28] Zhang YJ, Li YK, Yang XF. Route optimization algorithm for minimum fuel consumption of wind-assisted ship. J Appl Sci 2013;13(21):4805–11.
[29] Marie S, Courteille E. Sail-assisted motor vessels weather routing using a fuzzy logic model. J Mar Sci Technol 2013;19(3):265–79.
[30] Pètrès C, Romero-Ramirez MA, Plumet F. A potential field approach for

reactive navigation of autonomous sailboats. Robot Autonom Syst 2012;60(12):1520–7.
[31] Deng YJ, Zhang XK, Zhang GQ, Huang CF. Parallel guidance and event-triggered robust fuzzy control for path following of autonomous wing-sailed catamaran. Ocean Eng 2019;190:106442.
[32] Wang K, Xu H, Li JY, Huang LZ, Ma RQ, Jiang XL, Yuan YP, Mwero NA, Sun PT, Negenborn RR, Yan XP. A novel dynamical collaborative optimization method of ship energy consumption based on a spatial and temporal distribution analysis of voyage data. Appl Ocean Res 2021;112:102657.
[33] Wang K, Yan X, Yuan Y, Jiang X, Lin X, Negenborn RR. Dynamic optimization of ship energy consumption considering time-varying environmental factors. Transport Res Transport Environ 2018;46:81–93.
[34] Holtrop J, Mennen GGJ. An approximate power prediction method. Int Shipbuild Prog 1982;29(7):166–70.
[35] Kwon YJ. Speed loss due to added resistance in wind and waves. Nav Archit 2008;3:14–6.
[36] International Towing Tank Conference (ITTC). Full scale measurements speed and power trials analysis of speed/power trial data. In: Kgs. Lyngby, Denmark: international towing Tank conference (ITTC); 2005. 2005.
[37] Molland AF, Turnock SR, Hudson DA. Ship resistance and propulsion. Propel Charact 2011;10.1017/CBO9780511974113(12):261–95.
[38] Wang K, Yan XP, Yuan YP, et al. Optimizing ship energy efficiency: application of particle swarm optimization algorithm. Proc IME M J Eng Marit Environ 2018;232:379–91.
[39] HULL DESIGNING DEPARTMENT TECHNICAL DIVISION of NANTONG COSCO KHI SHIP ENGINEERING CO., LTD. In: The technical document of the particulars of the hull part of the designed ship [R]; 2015.
[40] Yan XP, Wang K, Yuan YP, et al. Energy efficient shipping: an application of big data analysis in engine speed optimization of inland river ships considering multiple environmental factors. Ocean Eng 2018;169:457–68.
[41] IMO. Guidelines for voluntary use of the ship energy efficiency operational indicator (EEOI). MEPC.1/Circ 17 August 2009;684.